The phonon mechanism explanation of the superconductivity dichotomy between FeSe and FeS monolayers on STO and other substrates.

Baruch Rosenstein¹ and B. Ya. Shapiro²

¹ Electrophysics Department, National Yang Ming Chiao Tung University, Hsinchu 30050, Taiwan, R. O. C*

² Physics Department, Bar-Ilan University, 52900 Ramat-Gan, Israel[†]

It was observed recently (K. Shigekawa et al, PNAS 116, 2470 (2019)) that while monolayer iron chalcigenide FeSe on $SrTiO_3$ (STO) substrate has a very high critical temperature, its chemical and structural "twin" material FeS/STO has a very low T_c if any. To explain this the substrate interfacial phonon model of superconductivity in iron chalcogenides is further developed. The main glue is the oxygen ion $\Omega_s = 60mev$ vibrations longitudinal optical (LO) mode. The mode propagates mainly in the TiO_2 layer adjacent to the monolayer (and genrally present also in similar highly polarized ionic crystals like $BaTiO_3$, rutile, anatase). It has stronger electron - phonon coupling to electron gas in FeSe than a well known $\Omega_h = 100mev$ harder LO mode. It is shown that while (taking into account screened Coulomb repulsion effects) the critical temperature of FeSe on STO and TiO_2 is above 65K, it becomes less than 5K for FeS due to two factors suppressing the electron - phonon coupling. The effective mass in the later is twice smaller and in addition the distance between the electron gas in FeSe to the vibrating substrate oxygen atoms is 15% smaller than in FeS reducinng the central peak in electron-phonon interaction. The theory is extended to other ionic insulating substrates.

PACS numbers: PACS: 74.20.Fg, 74.70.Xa,74.62.-c

Introduction. Several years ago a group of 2D high T_c superconductors $(T_c > 65K)$ was fabricated by deposition of a single unit cell (1UC) layer of FeSe on insulating substrates $SrTiO_3$ (STO) [1], TiO_2 (both rutile[2] and anatase[3]) and[4] $BaTiO_3$. The 3D parent iron chalcogenide (Se, S, Te) are unconventional superconductors (s^{\pm} wave symmetry) with modest $T_c = 5 - 10K$. Band structure is similar to that of iron pnictides suggesting a "nonconventional" spin fluctuation (SF) pairing mechanism within the FeSe layer[5]. However strong $^{16}O \rightarrow ^{18}O$ isotope substitution effect[6] in 1UC FeSe/STO indicates that superconductivity is at least enhanced by the electron - phonon interaction[7–11] (EPI). The relevant phonon is the oxygen ions vibrations in the interface layers. The role of the insulating substrate therefore clearly extends beyond the efficient monolayer charging[12].

Recently the second monolayer iron chalcogenide, FeS, on STO was synthesized[13] by the topotactic reaction and molecular-beam epitaxy. In both iron chalcogenides Fermi surface consists of two nearly coincident pockets around the M point of the Brillouin zone (BZ), while the electron pocket at Γ point of the parent material sinks (about 80meV) below Fermi level[14]. Despite the fact that (i) the bulk T_c , (ii) the 2D electron gas (2DEG) including spin dynamics, and (iii) EPI in FeSe and FeS are quite similar, superconductivity in FeS/STO was not observed[13] at least at temperatures above 10K. This came as a surprise and even was termed by the authors "a dichotomy" that "strongly suggests that the cross-interface electron–phonon coupling enhances T_c only when it cooperates with the pairing interaction inherent to the superconducting layer". This interpretation rules out theories in which the EPI is the major cause of the tenfold enhancement of T_c in FeSe/STO.

However despite the above superficial observations there are two important differences between the two monolayers. First the ARPES measurement[13] clearly demonstrates that the effective mass m^* that is twice larger in FeSe than in FeS. In addition the scanning transmission electron microscopy image of FeS/STO reveals that distance from the 2DEG gas in FeS to the vibrating substrate oxygen atoms, see Fig.1, is d=5.3A, larger than the corresponding distance[15] in FeSe/STO, d=4.6A. These two observations are in direct contradiction with statements (iii) above that the EPI is similar in two systems. Indeed since the EPI has a central peak in scattering (SCP) that exponentially depends on d, one would expect reduced EPI strength λ in FeS. The density of states in 2DEG is m^*/π , also reducing λ in FeS. On the contrary if the in - plane SF mechanism of pairing is similar and dominant, absence of superconductivity in FeS/STO poses a problem for this explanation.

In this letter the dichotomy between the iron chalcogenides monolayers FeSe and FeS is addressed theoretically in the framework of the phonon mechanism. The interfacial phonon is considered as the dominant superconductivity "glue" overcoming (the screened) Coulomb interaction. Systems of various effective masses m^* , the 2DEG layer substrate spacing d and dielectric constant of the substrate material are considered. We conclude that the dichotomy between superconductivity in FeSe/STO and FeS/STO is resolved within this framework.

Model. As mentioned above most of the theories of high T_c in FeSe monolayers[11, 16] are a variant of the incipient band SF model with the phonon pairing "boosting" T_c from 40K - 47K up (we are not aware of a similar considerations for the FeS). The EPI is represented by an interfacial mode of high frequency $\Omega = 100 mev$ close to that of the Fuchs - Kliewer modes (FK), observed via high resolution electron energy loss spectroscopy[17]. The FK are vibrations of the substrate oxygen atoms in the direction z perpendicular to the interface, see the blue arrow in Fig.1. The EPI strength $\lambda = 0.1$ turned out to be sufficient[11] to enhance the incipient band theory value of $T_c = 47K$ to $T_c = 65K$. If the spin fluctuations were switched off (U = 0), one would require at least $\lambda = 0.2$ (consistent with previous purely phononic calculations of ref. [7, 10]).

The identification of the phononic "glue" is a delicate task[16]. It was noted long ago[18] that transverse modes (including the FK mode responsible for the replica band in ARPES experiments[19]) are generally unable to provide the pairing glue, so that one has to concentrate on the longitudinal modes only. Multitude of both the bulk STO and the interface modes has been studied in the framework of the DFT [20]. A simple phenomenological model of ionic crystal allowed us[10] to identify two longitudinal optical (LO) surface modes that have the strongest coupling to 2DEG in a sense that their exchange produces effective attraction of electrons in the lateral (x-y) direction. These are the Ti-O stretching (along the surface, see black arrow Fig.1) mode comparable in energy of the FK, $\Omega_{st}^{LO} = 100 mev$, and a lower frequency Ti-O-Ti bending (still along the interface direction, see dark green arrow) mode $\Omega_b^{LO} = 60 mev$. Their matrix elements with the 2DEG electrons are about the same. All the other modes (including phonons in the FeSe layer itself) have negligible matrix elements.

Since the phononic glue comes mostly from the TiO_2 substrate separated from the 2DEG by the (minimal) distance d, see Fig. 1, the EPI coupling exhibits the exponential forward scattering peak [9]:

$$g(\mathbf{k}) \approx \frac{2\pi}{a} e^{-kd}.$$
 (1)

Here a is the lattice spacing, see Fig.1. The TiO_2 layer generally appears in all the substrates[15] (rutile, anatase, $STO, BaTiO_3$) as the first interface oxide layer (in addition to STO). The phonon exchange generate effective electron

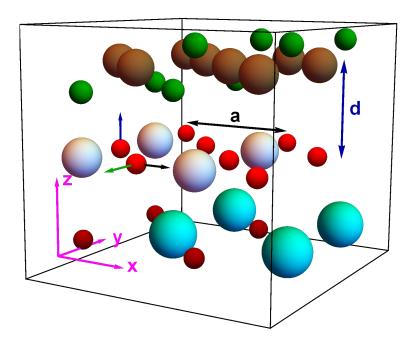


FIG. 1. Interfacial phonon modes. Oxygen ion's vibrations in the TiO_2 substrate layer (Ti - silver, O - red). The displacement in derection perpendicular (z axis, blue arrow) to the one unit cell thin Fe (brown) - chalcogenite (Se, S, Te - green) layer are associated with FK modes. The two modes most relevant for the phonon mediated pairing longitudinal optical modes are the Ti - O stretching mode (shown by black arrow) and the Ti - O - Ti bending (dark green arrow). The next layer Bi (cyan) - O (dark red) influencing the interfacial phonon frequency is also shown. Direction of the vibration wave is assumed to be along the x direction.

- electron attraction dynamic "potential" is

$$V_{\mathbf{k},n}^{ph} = -\frac{\left(Ze^2\right)^2}{M} \frac{g_{\mathbf{k}}^2}{\omega_n^2 + \Omega_s^2}.$$
 (2)

Here M and $Z\simeq 1.27$ are the oxygen ion mass and the ionic charge respectively[21] and $\omega_n=2\pi Tn$ is the bosonic Matsubara frequency. It was shown in ref.[10] that the lower frequency bending mode ($\Omega_b^{LO}=60meV$) leads to larger $\lambda=0.23$ than the stretching mode ($\Omega_{st}^{LO}=100meV$) with $\lambda=0.07$. Moreover the bending mode pairing alone is strong enough to mediate high T_c above 47K. This implies that the spin fluctuation contribution to pairing in the present case might be subdominant. This statement is not at odds with the understanding that the $T_c=8K$ superconductivity in bulk FeSe or FeS is due to SF, since there are two major differences between the bulk and 1UC. First the hole band at Γ in bulk disappears below Fermi surface and second the recent spin susceptibility measurement[22] from bulk to monolayer FeSe signal of the spin is completely different. Therefore it will be neglected in the present work. In view of the exponential SCP, Eq.(1), the EPI pairing in FeS/STO is weaker than in FeSe/STO since the distance between 2DEG and the TiO_2 layer increases[13] by15%. This alone should reduce the EPI coupling. To describe

the electron gas it is sufficient for our purposes to use a parabolic approximation for two M point bands of both

systems, $E_{\mathbf{k}} = k^2/2m^* - \mu$. Effective masses are $m_{FeSe}^* = 3m_e$ and $m_{FeSe}^* = 1.5m_e$ respectively, while Fermi energies are $\mu_{FeSe} = 60meV$ and $\mu_{FeS} = 30meV$ (values for FeS are deduced from the ARPES measurement[13]). The Fermi momentum $k_F = \sqrt{2m^*\mu}$ is nearly the same. As mentioned above the reduced density of state also suppresses the EPI pairing. As a result of the two facts for the weaker pairing in FeS/STO one should take into account the pseudo-potential[23]. Coulomb repulsion in 2DEG (although effectively screened by the dielectric substrate[7] in both monolayers), might completely suppress superconductivity.

The screened potential within RPA in the presence of the semi - infinite dielectric slab is

$$V_{\mathbf{k},n}^{C} = \frac{v_{\mathbf{k},n}^{C}}{1 - 2v_{\mathbf{k},n}^{C}\Pi_{\mathbf{k},n}}; \quad v_{\mathbf{k},n}^{C} = \frac{2\pi}{\varepsilon(\omega_{n})k},$$

$$(3)$$

where the (Matsubara) dielectric function inside the substrate reads[11]:

$$\varepsilon(\omega) = \frac{1}{2} \left\{ 1 + \varepsilon_{\infty} + (\varepsilon_0 - \varepsilon_{\infty}) \frac{\Omega_T^2}{\Omega_T^2 + \omega^2} \right\}. \tag{4}$$

Dielectric constants will be taken as follows. The optical value is rather universal for all the substrates (STO, rutile, anatase) $\varepsilon_{\infty} = 5.5$, while the static ε_{0} varies from as high as $\varepsilon_{0} = 3000$ for $SrTiO_{3}$ to $\varepsilon_{0} = 50$ for some anatase samples). The (bulk) transverse mode frequency appearing in Eq.(4) is estimated using the Lydanne-Sacks-Teller relation $\Omega_{T} = \Omega_{LO} \sqrt{\varepsilon_{\infty}/\varepsilon_{0}}$ with $\Omega_{LO} = 120 meV$.

The 2D Matsubara polarization function due the two nearly degenerate electron bands is:

$$\Pi_{\mathbf{k},n} = -\frac{m^*}{\pi} \left\{ 1 + 2 \operatorname{Re} \left(\left(1/2 + i\omega_n m^*/k^2 \right)^2 - \left(k_F/k \right)^2 \right)^{1/2} \right\}.$$
 (5)

The sum of two competing contributions the effective electron - electron interaction, $V_{\mathbf{k},n} = V_{\mathbf{k},n}^{ph} + V_{\mathbf{k},n}^{C}$, determines the superconducting properties of these systems.

The STM experiments[24] demonstrate that the order parameter is gapped (hence no nodes) and indicate a weakly anisotropic spin singlet pairing. Therefore we look for solutions for the normal and the anomalous Green's function of the Gorkov equations (derived for a multi - band system in ref. [10]), in the form $\left\langle \psi_{\mathbf{k},n}^{\rho} \psi_{\mathbf{k},n}^{*\sigma} \right\rangle = \delta^{\sigma\rho} G_{\mathbf{k},n}$, $\left\langle \psi_{\mathbf{k},n}^{\sigma} \psi_{-\mathbf{k},-n}^{\rho} \right\rangle = \varepsilon^{\sigma\rho} F_{\mathbf{k},n}$ (σ, ρ are spin components). In terms of the gap function,

$$\Delta_{\mathbf{k},m} = T_c \sum_{\mathbf{p},n} V_{\mathbf{k}-\mathbf{p},m-n} F_{\mathbf{p},n},\tag{6}$$

linearized gap equation becomes (normal Green's function not renormalized significantly at weak coupling),

$$-T_c \sum_{\mathbf{l},m} \frac{V_{\mathbf{l},n-m}}{\left(\omega_m^e\right)^2 + \left(E_{\mathbf{l}+\mathbf{q}} - \mu\right)^2} \Delta_{\mathbf{l}+\mathbf{q},m} = \Delta_{\mathbf{q},n},\tag{7}$$

where fermionic Matsubara frequency is $\omega_m^e = \pi T (2m+1)$. The angle (between **l** and **q**) integration can be performed for an conventional s-wave solution (observed in experiment[24]) leading to a simplified eigenvalue problem:

$$\frac{T_c m^*}{\pi} \sum_{m} \frac{1}{\omega_m^e} \left\{ \frac{\left(2\pi Z e^2\right)^2}{M} \frac{f_{ph} \left(\omega_m^e / 4\mu\right)}{\left(\omega_{n-m}^b\right)^2 + \Omega^2} - f_C \left(\frac{|\omega_m^e|}{4\mu}, \frac{|\omega_{n-m}^b|}{4\mu}\right) \right\} \Delta_m = \Delta_n.$$
(8)

The integrals (over $l \equiv |\mathbf{l}|/2k_F$) for the phonon and Coulomb contributions are defined as,

$$f_{ph}(z) = \int_{l=0}^{1} e^{-(4k_F d)l} R(z, l);$$

$$f_C(y, z) = \pi \int_{l=0}^{1} R(z, l) \left\{ \varepsilon (4E_F y) \frac{k_F l}{e^2} + 2m^* \left(1 + l^{-2} \sqrt{(l^2 + iy)^2 - l^2} \right) \right\}^{-1},$$
(9)

where $R(z, l) = \text{Re}(1 + z^2/l^2 - 2i|z| - l^2)^{-1/2}$.

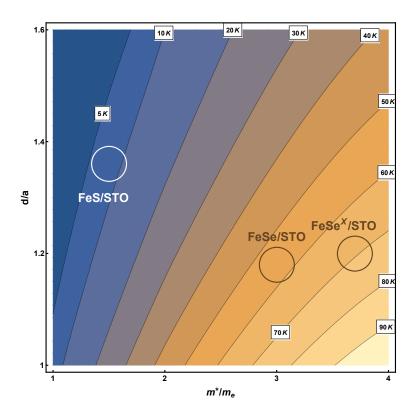


FIG. 2. Superconductivity critical temperature as function of effective mass and the distance between the iron chalcogenite layer and the interface TiO_2 (where the relevant phonon modes originate). The dielectric constant $\varepsilon_0 = 3000$ is fixed to represent $SrTiO_3$.

Critical temperature is obtained when the largest eigenvalue of the matrix of the linear Eq.(8) is 1. This was done numerically by limiting variable n to |n| < 200. The numerical results are presented in Figs. 2 and 3 for values of the bulk substrate dielectric constant $30 < \varepsilon_0 < 10000$. The range of effective masses is $m_e < m^* < 4m_e$, while the distance (in units of the lattice spacing a) between the conducting layer and the vibrating oxygen atoms is 1 < d/a < 1.6.

Results. The dependence of the critical temperature on the effective mass m^* and the distance between the 1UC iron chalcogenide and underlying TiO_2 interface layer is given in Fig. 2. It explains the dichotomy between a very high T_c in FeSe/STO and a very low T_c (10K or less) in FeS/STO. An approximate location of the two cases is indicated by two circles. The dielectric constants are fixed on the STO values mentioned above. It demonstrates that both the reduction of the effective mass and (to a lesser degree) the distance d difference contribute to the suppression of superconductivity in FeS/STO. In addition a higher effective mass 1UC strained FeSe epitaxially grown on $Nb: SrTiO_3/KTaO_3$ heterostructures[25] is marked as $FeSe^X$. For $T_c > 50K$ the dependence is approximately linear $T_c[K] = 18m^*/m_e - 22d \left[\mathring{A}\right] + 114$.

Critical temperature as function m^* of 1UC FeSe on ionic substrates with various dielectric constant is shown in Fig.3. The ratio d/a is fixed at 1.1. Dependence on the dielectric constant is due to screening of the Coulomb interaction. The pseudo - potential becomes important for low T_c . High $\varepsilon_0 = 3000$ STO and two relatively low ε forms of TiO_2 , rutile and anatase, are shown.

Discussion and conclusions. To summarize the interfacial LO phonon pairing theory in 1UC iron chalcogenides FeCh (Ch = Se, S, Te) on polar insulator ($SrTiO_3, TiO_2$) substrates is presented including the Coulomb pseudopotential effects. The LO modes originates in the TiO_2 layer of the substrate adjacent to the 1UC FeCh. The theory predicts three following tendencies leading to high critical temperature T_c . To achieve high critical temperature one

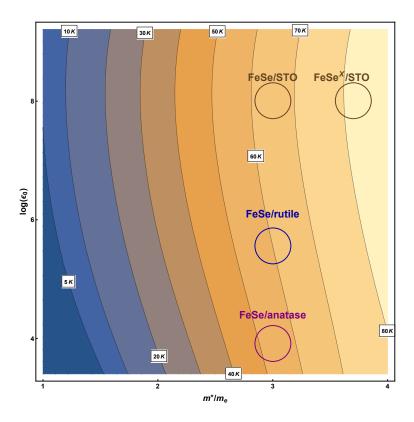


FIG. 3. Critical temperature as function of effective mass and dielectric constant (logarithmic scale). The distance between the iron chalcogenite layer and the interface TiO_2 d is fixed at 1.1a. Strongly dielectric material STO and moderately dielectric TiO_2 forms rutile ($\varepsilon_0 = 300$) and anatase ($\varepsilon_0 = 300$) are marked.

requires (i) small spacing between the electron gas inside the FeCh layer and the TiO_2 interfacial layer maximizing the strength of the electron - phonon coupling, (ii) high effective mass of the electrons in FeCh maximizing DOS, (iii) large dielectric constant ε_0 minimizing the Coulomb repulsion (pseudo-potential) effects. These three effects explain why FeSe/STO has very high T_c , while FeS/STO has very low T_c , if any. In addition it explains relative strength of pairing in FeSe on $BaTiO_3$, rutile and anatase structures of TiO_2 .

Let us put the interfacial theory of superconductivity in iron chalcogenides on ionic crystals in a more general framework of superconductivity in iron based materials. 3D pnictides like FeAs and 3D iron chalcogenides like the parent compounds FeSe or FeS generally have two features. The superconductivity is not the "plain" s - wave observed[24] in 1UC $FeCh/TiO_2$. It changes sign and is explained by the SF multiband model[5]. It is crucial that in addition to an electron band at M there exists also an electron band at Γ . In addition typically one often observes orbital selective Mott transition further favouring SF pairing (usually s^{\pm}) mechanism. It is not easy to modify these models to the plain s - wave gap typical to low T_c metals. The basic idea is still to utilize the hole pocket that is no about 100meV below Fermi surface[5, 11, 16] (the incipient band). Similar problem exists in explaining relatively high (T_c up to 48K) superconductivity in several 3D modifications of FeCh. These materials, including[26] metal intercalated (up to 48K) FeSe, $A_xFe_{2-y}Se_2$ (A=K, Sb, Li), and organic intercalations[27] like $Li_x(NH_2)_y(NH_3)_{1-y}Fe_2Se_2$, (Li, Fe)OHFeSe (up to 30K) and electric field induced superconductivity (48K) in FeSe [28] all exhibit s-wave pairing and only electron bands. It is plausible that bulk phonons also might provide a "glue" for the s - wave pairing. Therefore the pairing glue for the three groups of superconducting materials might be different. They are interface phonons for FeSe/STO, SF for iron pnictides and parent iron chalcogenides and either SF/3D phonon for intercalated iron chalcogenides.

Note that often the T_c enhancement in all three kinds of systems is attributed to "charging" [12] of the conducting layers by either electric field, intercalation (internal pressure). As the present work demonstrates, since in 2D the

pairing depends strongly on density of states (on Fermi level), the charging argument is effective only for 3D electron gas. In 2D DOS depends on effective mass only, $D \propto m^*/\hbar^2$. Charging mostly shifts the chemical potential and for fixed m^* increases DOS only in 3D: $D \propto m^{*3/2} \mu^{1/2}/\hbar^3$.

Acknowledgements.

We are grateful Prof. L. Wang, G. He, J.D. Guo, D. Li, J.J. Lin, J.Y. Lin for helpful discussions. Work of B.R. was supported by NSC of R.O.C. Grants No. 98-2112-M-009-014-MY3.

- * vortexbar@yahoo.com
- † shapib@biu.ac.il
- Q.-Y. Wang, et al, Chin. Phys. Lett. 29, 037402 (2012); D. Liu, et al, Nature Com. 3, 931 (2012); S. He, et al, Nature Mater. 12, 605 (2013); Q. Wang, et al, 2D Mater. 2, 044012 (2015).
- [2] S. N. Rebec, T. Jia, C. Zhang, M. Hashimoto, D.-H. Lu, R. G. Moore, and Z.-X. Shen, Phys. Rev. Lett., 118, 167002 (2017).
- [3] H. Ding et al. Phys. Rev. Lett., **117**, 067001 (2016).
- [4] R. Peng et al, Nat. Com. 5, 5044 (2014).
- [5] A. Kreisel , P. J. Hirschfeld and B. M. Andersen, Symmetry 12, 1402 (2020); F. Schrodi, A. Aperis, and P. M. Oppeneer, Phys. Rev. B 102, 014502 (2020).
- [6] Q. Song et al, Nature Com. 10, 758 (2019).
- [7] B. Rosenstein, B.Ya. Shapiro, I. Shapiro, and D. Li, Phys. Rev. B 94, 024505 (2016).
- [8] L. Rademaker, Y. Wang, T. Berlijn and T. Johnston, New J. Phys. 18, 022001 (2016); Y. Wang, K. Nakatsukasa, L. Rademaker, T. Berlijn and S. Johnston, Supercond. Sci. Technol. 29, 054009 (2016).
- [9] M. L. Kulić and O. V. Dolgov, New J. Phys. 19, 013020 (2017); M. L. Kulić, Phys. Rep. 38, 1 (2000).
- [10] B. Rosenstein, B.Ya. Shapiro, Phys. Rev. B 94, 024505 (2016).
- [11] F. Schrodi, A. Aperis, and P. M. Oppeneer, Phys. Rev. B **102**, 180501 (2020); L. Rademaker, G. Alvarez-Suchini, K. Nakatsukasa, Y. Wang, and S. Johnston, "Enhanced superconductivity in FeSe/SrTiO3 from the combination of forward scattering phonons and spin fluctuations", arXiv:2101.08307v1 (2021).
- [12] L. Wang X, Ma, and Q. K. Xue, Supercond. Sci. Technol. 29, 123001 (2016).
- [13] K. Shigekawa, K. Nakayama, M. Kuno, G. N. Phana, K. Owada, K. Sugawara, T. Takahashi, and T. Sato, PNAS, 116, 24470 (2019).
- [14] "Origin of the Electronic Structure in Single-Layer FeSe/SrTiO3 Films", D. Liu, X. Wu, F. Li, Y. Hu, J. Huang, Y. Xu, C. Li, Y. Zang, J. He, L. Zhao, S. He, C. Tang, Z. Li, L. Wang, Q. Wang, G. Liu, Z. Xu, X.-C. Ma, Q.-K. Xue, J. Hu, and X. J. Zhou, Arxiv 2012.09032 (2020).
- [15] F. Li et al, 2D materials, **3**, 024002 (2016).
- [16] Y. Bang, Sci. Rep., 9, 3907 (2019).
- [17] S. Zhang et al, Phys. Rev. B 94, 081116 (2016); S. Zhang, Phys. Rev. B 97, 035408 (2018); X. Xu, S. Zhang, X. Zhu and J. Guo, J. Phys. Cond. Mat. 32 343003 (2020).
- [18] L. P. Gorkov, Phys. Rev. B, 060507(R) (2019).
- [19] F. Li and G. A. Sawatzky, Phys. Rev. Let. 120, 237001 (2018).
- [20] L. Zhao et al, Nature Com. 10, 1038 (2016); B. Li, Z. W. Xing, G. Q. Huang, and D. Y. Xing, J. Appl. Phys. 115, 193907 (2014); Y. Wang, A. Linscheid, T. Berlijn, and S. Johnston, Phys. Rev. B 93, 134513 (2016).
- [21] R. A. Evarestov, "Quantum Chemistry of Solids", Second Edition, Springer Series in Solid-State Sciences 153, Springer, London, 2012.
- [22] J. Pelliciari et al, "Evolution of spin excitations from bulk to monolayer FeSe", arXiv:2008.09618v1 (2020).
- [23] W.L. McMillan, Phys. Rev. 167, 331 (1968).
- [24] Q. Fan, et al, Nature Phys., 11, 946 (2015); C. Tang et al, Phys. Rev. B 93, 020507 (2016).
- [25] R.Peng et al., Phys. Rev. Lett. 112, 107001 (2014).
- [26] J. G. Guo, S. F. Jin, G. Wang, S. C. Wang, K. X. Zhu, T. T.Zhou, M. He, and X. L. Chen, Phys. Rev. B 82, 180520R (2010); A. F. Wang et al., Phys. Rev. B 83, 060512(R) (2011); M. Z. Shi et al. Phys. Rev. Materials 2, 074801 (2018).
- [27] M. Burrard-Lucas et al., Nat. Mater. 12, 15 (2013); X. F. Lu et al., Nat. Mater. 14, 325 (2015).
- [28] B. Lei et al, Phys. Rev. Let. 116, 077002 (2016).